ACS OMEGA

http://pubs.acs.org/journal/acsodf

Article

Progeny Transfer Effects of Chitosan-Coated Cobalt Ferrite Nanoparticles

Md Salman Shakil,* Md. Forhad Uddin, Md. Reaz Morshed, Md Simul Bhuiya, Morshed Alam, Md. Sakib Hossen, Mahruba Sultana Niloy, Mohammad Mahfuz Ali Khan Shawan, Sheikh Manjura Hoque, and Md. Ashraful Hasan*

Cite This: *ACS Omega* 2023, 8, 15152−15159

Read Online

ACCESS | Metrics & More | Article Recommendations | Supporting Information

ABSTRACT: Cobalt ferrite nanoparticles (CFNs) are promising materials for their enticing properties for different biomedical applications, including magnetic resonance imaging (MRI) contrast, drug carriers, biosensors, and many more. In our previous study, a chitosan-coated CFN (CCN) nanocomplex demonstrated potential as an MRI contrast dye by improving the biocompatibility of CFN. In this study, we report the progeny transfer effects of CCN following a single intravenous injection of CCN (20, 40, or 60 mg/kg) in pregnant albino Wistar rats. Biochemical and histological observation reveals that CCN is tolerated with respect to maternal organ functions (e.g., liver, kidney). Atomic absorption spectroscopy results showed that CCN or CCN-leached iron could cross the placental barrier and deposit in the fetus. Furthermore, this deposition accelerated lipid peroxidation in the placenta and fetus.

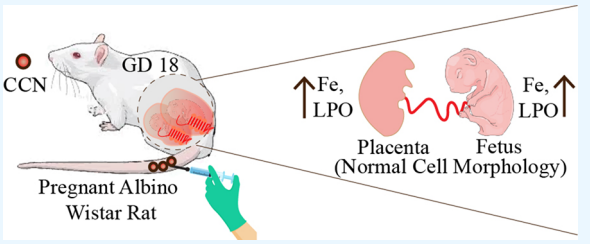

1. INTRODUCTION

Cobalt ferrite nanoparticles (CFNs) are magnetic nanoparticles that have unique physiochemical properties.[1] High magnetocrystalline anisotropy, saturation magnetization, and high coercivity are some of the special features of CFNs.[1,2] CFNs possess diverse biomedical applications including targeted drug delivery, biosensing, bioseparation, magnetic resonance imaging, and magnetic hyperthermia treatment.[1,2] Additionally, CFNs show anticancer, antimicrobial, and antioxidant activities.[3] Furthermore, conjugation of CFN with chitosan (CH) could enhance anticancer activity via synergistic actions.[3,4] However, one of the major concerns with CFN biomedical applications is its cytotoxic effect(s) in the in vivo system.[5] CH is a biocompatible polymer and coating of CFN with CH (i.e., chitosan-coated CFNs (CCNs)) enhances the biocompatibility of CFNs.[4,6] Therefore, previously, we synthesized CCNs to improve CFN biocompatibility.[6]

Nanomaterials may cross the placental barrier and induce developmental toxicity in the fetus.[7] Maternal−fetal transfer of nanoparticles including iron oxide[8−10] and nickel[11,12] has been confirmed in rodents. However, no study reported the transfer of CFNs or CCNs across the placenta in mice or rats and their effects on maternal body or fetus. deSouza et al. (2012)[13] reported that metal cobalt ions can cross the placental barrier in the pregnant female. Some studies confirmed the transplacental transport of iron oxide nanoparticles in mice[8−10,14] and rats.[15,16] Iron oxide-based magnetic mesoporous silica nanoparticles crossed the placenta and deposited in the fetus's lungs, liver, and intestine.[16] Vaginal instillation of magnetic iron oxide nanoparticles showed entry of nanoparticles in embryonic circulation through the umbilical cord.[14] On the other hand, the chitosan oligosaccharide (a CH derivative) showed toxicity on dams and teratogenic effects on albino rat fetuses.[17] Moreover, chitosan nanoparticles (CSNPs) induced structural and functional abnormalities in the placenta and affected embryo development by down-regulating responsible genes and also affected mitochondrial function.[18] Additionally, CSNPs caused embryo damage via oxidative or endoplasmic reticulum stress and autophagy.[19] More importantly, the drug metabolite of one organ could have toxic effects on other organs.[20] As a result, before theranostic use of CCN in pregnancy, it must be determined whether CCN crosses the placental barrier and what effects it may have on the maternal body and the fetus.

The placental crossing of CCNs and their potential consequences on the body of the mother or the fetus is yet to be documented. In this study, we attempted to assess the effects of CCNs on maternal organs and progeny transfer effects in a pregnant albino Wistar rat model.

Received: January 9, 2023
Accepted: April 5, 2023
Published: April 19, 2023

2. MATERIALS AND METHODS

2.1. CCN Synthesis and Characterization. CCNs were synthesized and characterized as described previously by Shakil et al. (2020).[6] Briefly, CFNs were synthesized using a coprecipitation method and coated with CH. CCNs were characterized by transmission electron microscopy, Fourier transform infrared (FTIR) and Raman spectra, differential scanning calorimetry (DSC), thermogravimetric analysis (TGA), dynamic light scattering (DLS), and surface charge (ζ potential) analysis (Table S1).[6]

2.2. Design of In Vivo Experiments. Healthy female albino Wistar rats (about 10 weeks old) were included in the current study. Rats were bred and reared in the animal house facility conditions of the Department of Biochemistry and Molecular Biology, Jahangirnagar University. The target values of room temperature and relative humidity (RH) were 25 ± 2 °C and 50−70% RH, respectively. The experimental rats were housed in plastic cages with 12 h light−dark cycle. The pregnant rats were provided with normal experimental pelleted animal food and drinking water ad libitum. The experiments were conducted following the institutional guidelines and approved by the Institutional Animal Ethical Committee, approval number BBEC, JU/M-2022(6)2. Albino Wistar male rats were allowed to mate with the experimental female rats under the animal facility conditions. Pregnancy was assured by the presence of a vaginal plug, and it was counted as gestational day 0. The pregnant females were separated from the other rats and received CCN injections on gestational day (GD) 18.[21]

The pregnant albino Wistar rats (200−220 g body weight) were monitored to observe any changes in fur, skin, excretions, and body weight for 0−48 h after an intravenous (IV) injection of CCNs (Table 1). While the control rats group received phosphate-buffered saline (PBS) through 26 G needles in the tail vein.

Table 1. Animal Groups and Experiment Dosage

group	dose[a]	frequency of dosage	animals
group 1	PBS	single intravenous injection	n = 6
group 2	CCN (20 mg/kg)		n = 6
group 3	CCN (40 mg/kg)		n = 6
group 4	CCN (60 mg/kg)		n = 7

[a]CCN: chitosan-coated cobalt ferrite nanoparticles.

Previously, Shakil et al. (2020)[6] examined the biocompatibility of CCNs up to a 20 mg/kg dose in male albino Wistar rat for 1−28 days. Assuming 20 mg/kg is a safe dose, acute effects of 1−3× dose was designed. Higher dosage (over 60 mg/kg) was avoided considering the fluid overload for the experimental rats.

Body weight of pregnant rats was monitored during the experimental period. At the end of 24 and 48 h post-treatment, three rats from each group were sacrificed to examine the histopathological changes, effects on organ function biomarkers, biodistribution, and cytotoxic effects. Animals received an intraperitoneal injection of ketamine (100 mg/kg) before sacrifice, and blood was withdrawn from the inferior vena cava. The blood sample was transferred in an anticoagulant-free test tube and centrifuged at 7000 rpm for 5 min. Serum was collected in small Eppendorf tubes for biochemical analysis. For histopathological examination, freshly collected placenta, fetus liver, and kidney were preserved in 10% formaldehyde solution for fixation, while the tissue samples for lipid peroxide (LPO) were perfused using 0.9% NaCl solution.

2.3. Histopathological Inspections. Tissue samples were processed as described previously by Shakil et al. (2020).[6] Liver, kidney, placenta, and fetus tissues were fixed in 10% buffered formalin. Then paraffin blocks were prepared and cut into thin tissue sections (4−5 μm) using a Leica rotary microtome (LIECA RM2235). These processed tissue sections were stained with routine hematoxylin and eosin (H&E) stain. A microscopic investigation was carried out using an Olympus DP72, Tokyo, Japan, microscope with normal spectra. Photomicrographs were taken at 400× using a digital camera connected to the microscope.

2.4. Biochemical Assessments. The activities of liver and kidney function biomarkers including alanine transferase (ALT), aspartate transferase (AST), alkaline phosphatase (ALP), albumin, blood urea nitrogen (BUN), uric acid, and creatinine were estimated by commercially available standard assay kits (Linear, Spain). While mineral concentrations (sodium and potassium) were determined by commercially available standard assay kits (Atlas, U.K.). Experimental reading was taken using a PD-303S spectrophotometer (APEL, Japan).

2.5. Determination of Iron Levels in Maternal Liver, Placenta, and Fetus. Liver, placenta, and fetus tissues were placed in an oven for 48 h (model OP100, LTE Scientific Ltd., Greenfield, Oldham, Great Britain) to dry at 65 °C. After being oven-dried, tissue samples were placed in a glass mortar for grinding. Wet digestion techniques were used to prepare all of the powdered samples, including liver, placenta, and fetus.[22] The sample was first weighed in the crucible using an analytical balance and digested using 10 mL of a mixture of 65% nitric acid and 70% perchloric acid (3:1). The solution was then cooked on a hot plate for 15−20 min at 150 °C until it was nearly dry, and it was then cooled for 5−10 min. After that, the cooled samples were diluted with 50 mL of distilled water, filtered through Whatman filter paper No. 1, and then kept in 50 mL of LDPE plastic bottles. Blank and standard solutions were also prepared. Iron (Fe) concentrations in maternal liver, placenta, and fetus were determined with an atomic absorption spectrometer (model AA-7000, Shimadzu, Japan).

2.6. LPO Assay. The oxidative stress of the maternal liver, placenta and fetus was examined by calculating the level of LPO. LPO was examined by testing the thiobarbituric acid reactive substances.[23,24] Briefly, the liver, placenta, and fetus homogenates (0.1 mL) were mixed with 0.1 mL of 8.1% (w/v) sodium dodecylsulfate, 2 mL of 0.4% thiobarbituric acid (dissolved in 20% acetic acid, pH 3.5), and 0.1 mL of distilled water. Each tube was then vortexed and put in heat blocker for 1 h at 95 °C. After that, tubes were cooled and a 1.5 mL of n-butanol/pyridine (15:1) mixture was added to each tube. Following this, the samples were vigorously vortexed for about 10 min and centrifuged for 10 min at 1200g. Then the supernatant was taken from each tube, and the absorbance was measured at 532 nm using a PD-303S spectrophotometer (APEL, Japan). In this assay, 1,1,3,3-tetraethoxypropane was used as the standard.

2.7. Data Analysis. Experimental results were analyzed using Prism-GraphPad 8 (USA). Data were presented as the mean ± SEM. The threshold for statistical significance was set at $p < 0.05$.

https://doi.org/10.1021/acsomega.3c00148
ACS Omega 2023, 8, 15152−15159

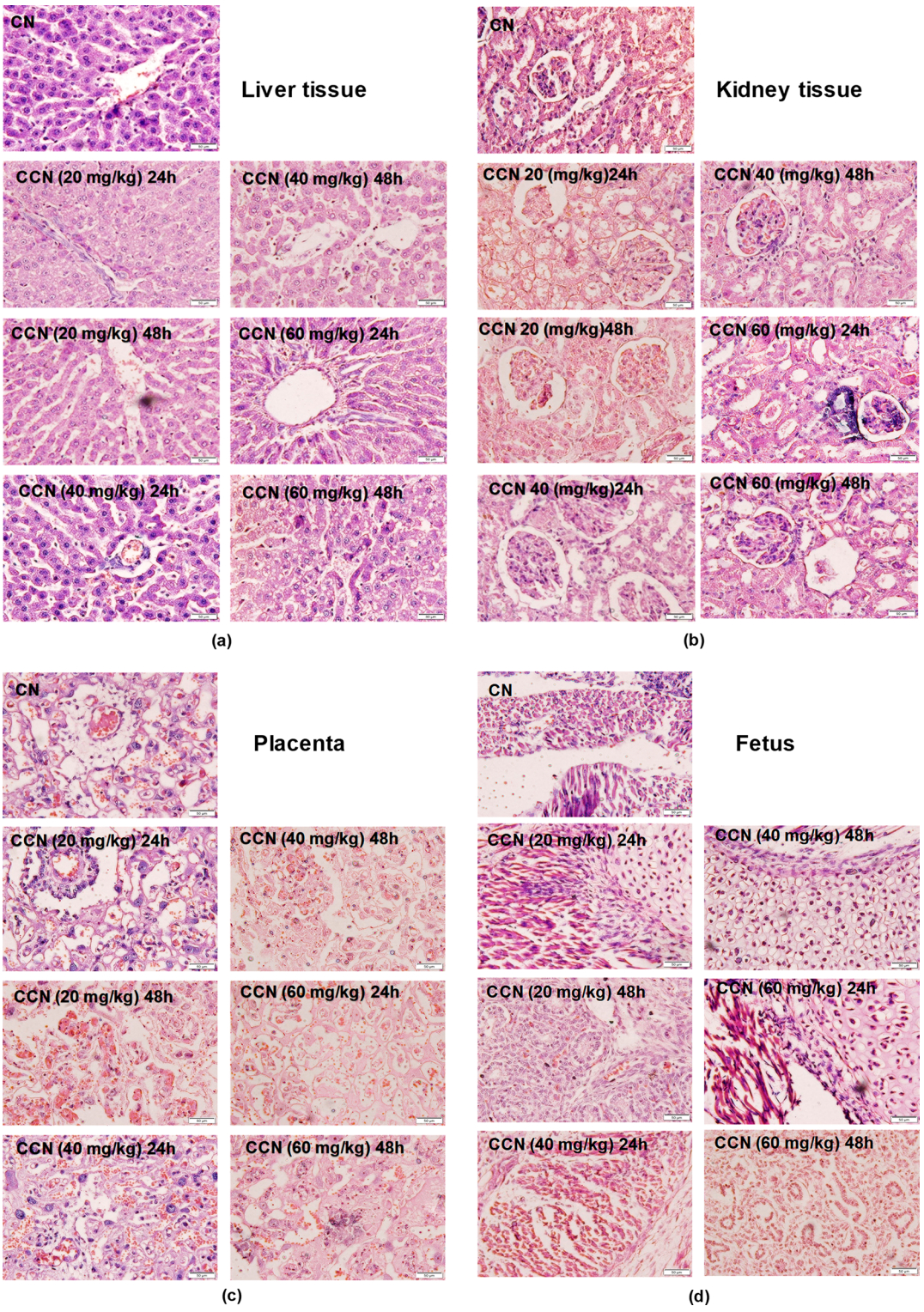

Figure 1. Histological images of the (a) liver, (b) kidney, (c) placenta, and (d) fetus. Sections of the (a) liver, (b) kidney, (c) placenta, and (d) fetus tissues were collected from the pregnant albino Wistar rats following 24 and 48 h of CCNs (20−60 mg/kg) postinjection. On the other hand, the CN group received an intravenous injection of PBS. Tissue samples were prepared with hematoxylin and eosin (H&E) stains. Any sign of tissue damage was not observed in the case compared to the control. Images were taken at 400×. CN, control; CCN, chitosan-coated cobalt ferrite nanoparticles.

3. RESULTS

3.1. MTS Assay. Cytotoxic activity of CCNs toward A172 glioblastoma cells was tested at 20 and 100 μg/mL from 24 to 72 h. MTS assay results indicated that CCNs did not show potent cytotoxic activity against A172 cells (Figure S1). Additionally, any concentration and time-dependent cytotoxic activity were not observed.

3.2. Physiological Parameters. There was no discernible difference in body weight among the groups during the

https://doi.org/10.1021/acsomega.3c00148
ACS Omega 2023, 8, 15152−15159

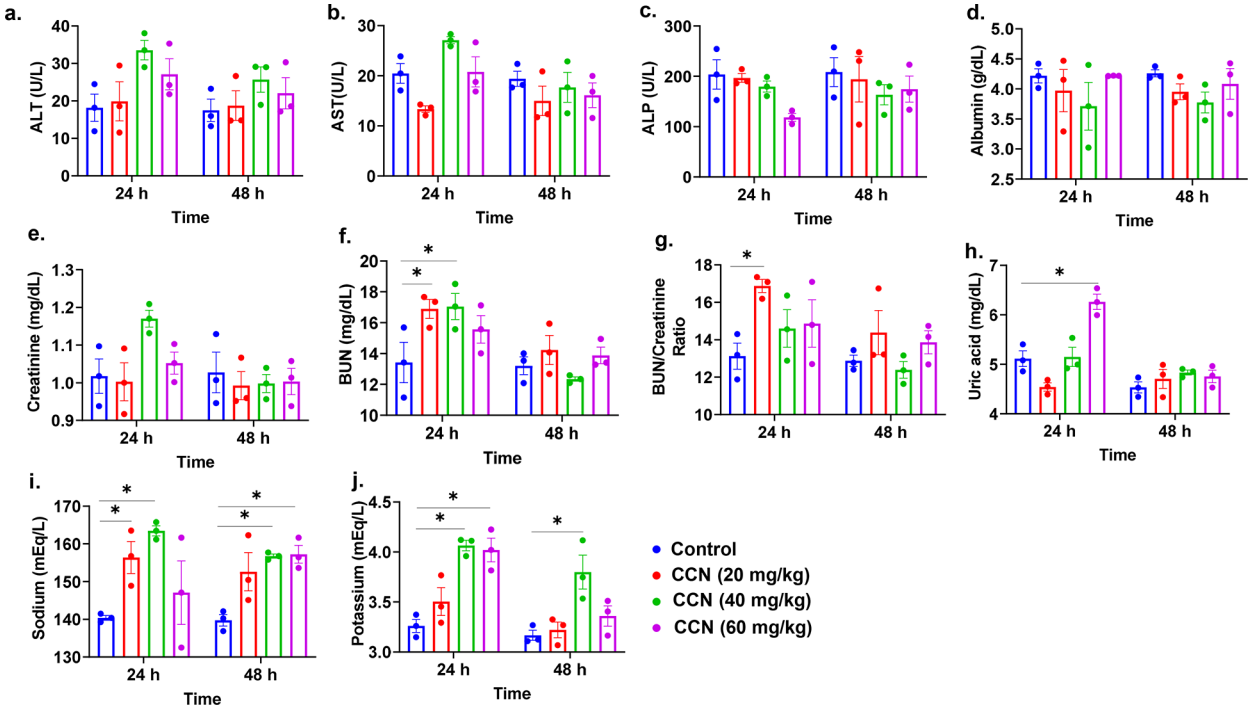

Figure 2. Time- and concentration-dependent effects of CCNs on biochemical parameters. Pregnant albino Wistar rats were sacrificed following 24 and 48 h of CCN (20−60 mg/kg) postinjection. ALT (a), AST (b), ALP (c), albumin (d), creatinine (e), BUN (f), uric acid (g), BUN/creatinine ratio (h), sodium (i), and potassium (j) concentration were calculated to detect the effect of CCNs on these biochemical parameters. Values are presented as mean ± SEM, three animals per group. Two-way ANOVA coupled with a Tukey's posthoc test was used to analyze experimental data. *$p > 0.05$, significantly different compared to control. CCN, chitosan-coated cobalt ferrite nanoparticles.

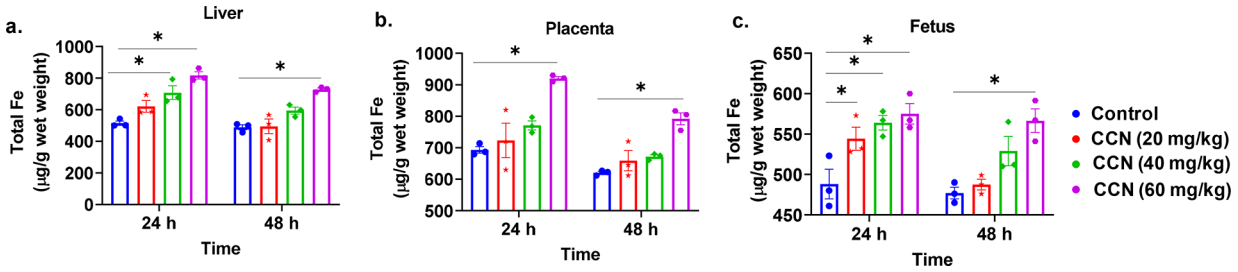

Figure 3. Time- and concentration-dependent clearance of iron from the liver, placenta, and fetus. Pregnant albino Wistar rats were sacrificed following 24 and 48 h of CCN (20−60 mg/kg) postinjection. AAS analysis was performed to detect the iron level in the liver (a), placenta (b), and fetus (c). Values are presented as mean ± SEM, three animals per group. Two-way ANOVA coupled with a Tukey's posthoc test was used to analyze experimental data. *$p > 0.05$, significantly different compared to control. AAS, atomic absorption spectroscopy; CCN, chitosan-coated cobalt ferrite nanoparticles.

treatment period (0−24 h) (Table S2). The pregnant animals resembled the control animals in terms of their physical appearance, food intake, and excretion. Additionally, no physical defects were seen in the fetus. One rat from the 60 mg/kg group died after 20 h of CCN treatment for an unknown reason, while no death cases were recorded in other groups.

3.3. Histopathological Changes. CCNs did not affect the histoarchitecture of the liver (Figure 1a). In the CCN-treated groups, necrotic death of the hepatocytes, fibrotic scarring, or hyperemia was not observed. More importantly, structures surrounding the central vein and hepatic sinusoids were devoid of hydropic degeneration. Furthermore, any type of glomerular injury, renal tubular damage, or marked swelling of the renal tubules was undetected in the treatment groups (Figure 1b). Additionally, like the control, the histoarchitecture of placental and fetus tissue was intact in the CCN treatment groups (Figure 1c,d).

3.4. Biochemical Changes. Liver function biomarker (ALT, AST, ALP, and albumin) levels were analyzed 24−48 h post-treatment of 20−60 mg/kg CCNs (Figure 2a−d). Changes in liver function biomarkers were not detected. Furthermore, creatinine level in this case compared to that in the control was not altered, indicating normal kidney function (Figure 2e). A significant change in BUN level was calculated in treatment groups 1 and 2 at 24 h (Figure 2f). Furthermore, the BUN/creatine level indicated that treatment group 1 at 24 h could have some impaired kidney function (Figure 2g). Similarly, uric acid levels increased only in the treatment group 3 (Figure 2h). More importantly, significant changes in the Na^+ ion level were calculated in the treatment group at a high concentration at 24 and 48 h, while the high concentration of CCNs caused a significant change in K^+ ion level at 24 h only

https://doi.org/10.1021/acsomega.3c00148
ACS Omega 2023, 8, 15152−15159

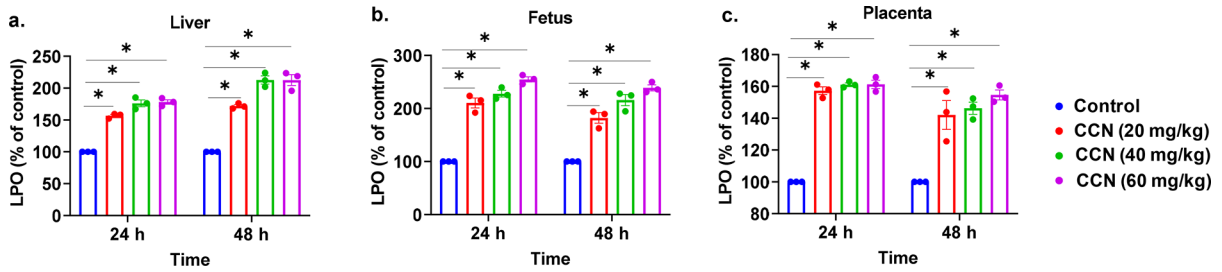

Figure 4. Time- and concentration-dependent lipid peroxidation of the liver, fetus, and placenta. Pregnant albino Wistar rats were sacrificed following 24 and 48 h of CCN (20−60 mg/kg) postinjection. LPO analysis was performed to detect the oxidative stress in the liver (a), fetus (b), and placenta (c). Values are presented as mean ± SEM, three animals per group. Two-way ANOVA coupled with a Tukey's posthoc test was used to analyze experimental data. *$p > 0.05$, significantly different compared to control. CCN, chitosan-coated cobalt ferrite nanoparticles.

(Figure 2i,j). Together, the results indicated that CCNs could have a nephrotoxic effect or impair the kidney filtration system.

3.5. Atomic Absorption Spectroscopy. Biodistribution of CCNs or CCNs leached iron in different maternal organs and fetus was detected using atomic absorption spectroscopy (AAS). In the treatment groups, a significantly high iron level was detected in the liver, placenta, and fetus (Figure 3a−c). The iron concentration in the placenta was higher than that in the fetus. Additionally, the iron level in the reported organs decreased over time. These findings indicated that CCN- or CCN-derived iron passed the placenta and reached the fetus.

3.6. LPO. Time- and concentration-dependent oxidative stress was observed in the liver, fetus, and placenta in the pregnant rats (Figure 4a−c). In our study, the LPO (nmol/mg protein) level of the liver, placenta, and fetus was significantly increased in CCN-treated (20−60 mg/kg) animals at 24 h. The same treatment also caused a significant increase of LPO in the liver and fetus at 48 h. Interestingly, the LPO of the placenta reduced to normal in the 20 mg/kg treatment group; however, at higher concentrations, significantly high LPO was also calculated at 48 h. The increase of oxidative stress in the treatment group might be due to the deposition of CCN- or CCN-leached Fe or Co.

4. DISCUSSION

We used previously synthesized CFNs (diameter: about 10 nm) using the chemical coprecipitation approach to conduct this study. The surface was modified with CH to enhance CFN biocompatibility. Additionally, Shakil et al. (2020)[6] confirmed that 10 mg/kg CCNs enhanced the MRI contrast efficiency in brain tissue imaging. In this study, we investigated the cytotoxic potential of CCN against A172 cells. Furthermore, pregnant albino Wistar rats were intravenously given three different dosages of CCN (20, 40, and 60 mg/kg) on gestation day 18 to study the effects of CCNs on progeny transfer and their biodistribution in the mother's organs (including liver and placenta) and the fetus's body.

According to the MTS experiment results, CCNs did not exhibit concentration- or time-dependent cytotoxicity against A172 cells (Figure S1). CCN decreased 10−20% of viability of A172 cells. Previously, Nahar et al. (2022)[25] reported that folate chitosan-coated CFNs decreased around 5% viability of human cervical cancer HeLa cells at a 500 μg/mL concentration. Furthermore, at a concentration of 6000 g/mL, the number of viable HeLa cells decreased by about 25%,[25] while CFNs displayed potent anticancer activity toward MCF-7 breast cancer and HepG-2 liver cancer cells with IC_{50} values of 45.12 and 61.86 μg/mL, respectively.[3] As some of the drug candidates including nanoparticles interact with 3-(4,5-dimethylthiazol-2-yl)-2,5-diphenyltetrazolium bromide dye and produce misleading results, assessing the cell viability using a sulforhodamine B assay could better represent CCN potency.[26]

Inside the human body, nanoparticles interact with various cellular organelles and induce cytotoxicity, genotoxicity, metabolic alteration, and cell death.[2] Additionally, smaller sized nanoparticles assist in higher absorption and longer bioavailability than bulkier counterparts, thus increasing their potential toxicity impact.[9] Exposure of nanoparticles during gestation causes complications in dams and developing fetuses.[27,28] Following treatment with 20−60 mg/kg CCNs, there were no noticeable changes in the pregnant animals' body weight (Table S2), appearance, food intake, or excretion. Treatment-linked alternations of maternal body weight, food consumption, gross findings, and morphological changes were not seen with silver or titanium oxide nanoparticles.[29,30]

Organ damage can be clinically evaluated by examining their organ-specific serum biomarkers and histopathological changes.[31,32] Histopathological results indicated that CCNs did not induce any morphological changes of maternal tissues (liver, kidney, placenta) and fetus tissues (Figure 1). Previously, it was reported that CCNs or CFNs are well-tolerated in liver and kidney tissues,[6,33] while Bassiony et al. (2022)[34] showed that magentic nanoparticles induce inflammatory cell infiltration and histological damage on liver and kidney tissues. Similarly, silver nanoparticles have been reported to damage the histoartitecture of fetus tissues.[35]

The primary organ involved in CFN detoxification is the liver.[36] Significant changes of liver function biomarkers (ALT, AST, ALP, and albumin) were not observed in treatment groups (20−60 mg/kg CCN) compared to the control at 24 and 48 h (Figure 2a−d). Previously, Shakil et al. (2020)[6] reported that CCNs (up to 20 mg/kg) were well-tolerated in the liver tissues of male albino Wistar rat following a single IV injection. Similarly, serum creatine level was not altered in the treatment groups, indicating normal kidney function (Figure 2e). However, the BUN level was significantly increased in treatment groups 1 and 2 at 24 h (Figure 2f). On the other hand, a significant change of the BUN/creatine level was observed only in the treatment group 1 at 24 h (Figure 3g). At the same time, the uric acid level increased only in treatment group 3 (Figure 2h). These findings indicate that CCNs could have a transient acute nephrotoxic effect as these biomarkers return to their normal level at 48 h. Previously, Akhtar et al. (2020)[37] reported that a single intraperitoneal injection of cube-shaped CFNs (100 mg/kg) in healthy albino rats

https://doi.org/10.1021/acsomega.3c00148
ACS Omega 2023, 8, 15152−15159

significantly increased liver (e.g., bilirubin, ALT, AST, ALP) and kidney (BUN, creatinine, urea) function biomarkers level at days 1 and 8. Interestingly, remarkable changes of sodium and potassium level were found in the treatment groups at 24 to 48 h (Figure 2i,j). It should be noted that dose-dependent effects were not observed in the current study. Previously, it has been reported that silver nanoparticles inhibit Na^+/K^+-ATPase,[38] and inhibition of Na^+/K^+-ATPase activity could have an effect on normal kidney function of pregnant rats,[39] while Wang et al. (2016)[22] reported that long-term exposure of zinc oxide nanoparticles had no effect on mineral metabolism.

The diameter of the uterine and placental blood vessels changes during normal placental development. During pregnancy, blood flow to the uterus is increased by 90-fold on GD 20. More importantly, approximately 6% of the cardiac output is distributed to the placentas on GD 20.[40] The liver also receives a considerable portion of the cardiac output (blood flow is 0.1 mL/min/g at GD18 and 0.07 mL/min/g at GD 20).[40] AAS results indicated that CCNs or CCN-derived iron deposits in the liver, placenta, or fetus (Figure 3). Additionally, the level of iron decreased over time, which might be due to the gradual clearance of CCNs from the animal's body.[6,41] It has been reported that silica (70 nm) nanoparticles accumulated in the placenta, and their concentration decreased after 24 h of IV injection, while 300 or 1000 nm silica nanoparticles were not observed in the placenta or fetus, indicating nanoparticle accumulation depends on particle size.[42] Deposition of iron oxide nanoparticles or Fe could increase the oxidative stress of maternal organ or the fetus.[9,43]

Oxidative stress is one of the major mechanisms of nanoparticle-mediated fetotoxicity.[27] CFNs increased reactive oxygen species generation and induced DNA damage, apoptosis, or impaired organ development.[44] An increase of LPO is an indicator of nanoparticle-mediated tissue damage.[45] CCN (positively charged)-induced increase in LPO indicates that LPO increased oxidative stress to maternal organs (liver), the placenta, and the fetus (Figure 4). Previously, it was reported that repetitive oral administration of silver nanoparticles caused oxidative stress to hepatic tissues. However, the same treatment did not induce any developmental toxicities in the fetus,[29] and Di Bona et al. (2015)[9] reported that iron oxide nanoparticles at a higher concentration (100 mg/kg) caused developmental toxicity. Interestingly, the damaging pattern was linked to surface charge, and positively charged nanoparticles induced greater damage compared to negatively charged ones.[9] Results of the current study indicated that CCN- or CCN-derived Fe passed the placental barrier and mediated oxidative stress in the fetus.

Previously, 10 mg/kg CCNs (human equivalent dose 1.62 mg/kg) showed promise for biomedical applications as a T_2 MRI contrast dye.[6] The current study indicated that if CCNs (20−60 mg/kg) are injected during pregnancy, a severe toxic effect might not be observed. However, as CCNs pass the placental barrier, their long-term effects on the maternal organs and the fetus need to be unveiled.

5. CONCLUSION

Contrary to expectations, CCNs did not exhibit significant anticancer effects against A172 cells. Additionally, a single IV administration of CCNs (20−60 mg/kg) had no discernible effects on the maternal liver. Although the histopathological results indicated that CCNs did not alter maternal renal function, biochemical data showed that CCNs might have an acute nephrotoxic effect. More importantly, the deposition of CCN- or CCN-derived Fe may trigger oxidative damage to both the mother's organs (such as the liver) and the developing fetus. Further research is needed to understand the long-term effects of CCNs on pregnant rats and their fetuses as these results are at odds with histopathological results.

■ ASSOCIATED CONTENT

Data Availability Statement

Data are included in the article or in the Supporting Information.

Supporting Information

The Supporting Information is available free of charge at https://pubs.acs.org/doi/10.1021/acsomega.3c00148.

Determination of cell viability; cytotoxicity of CCN in A172 cells (Figure S1); size, hydrodynamic diameter, ζ potential, and M_{max} of CCN (Table S1); effect of CCN on the body weight (g) of pregnant albino Wistar rats (Table S2); references (PDF)

■ AUTHOR INFORMATION

Corresponding Authors

Md Salman Shakil − *Department of Mathematics and Natural Sciences, Brac University, Dhaka 1212, Bangladesh;* orcid.org/0000-0002-8922-9500; Email: salman.shakil@bracu.ac.bd

Md. Ashraful Hasan − *Department of Biochemistry and Molecular Biology, Jahangirnagar University, Savar 1342, Bangladesh*; Email: ashrafulhasan@juniv.edu

Authors

Md. Forhad Uddin − *Department of Biochemistry and Molecular Biology, Jahangirnagar University, Savar 1342, Bangladesh*

Md. Reaz Morshed − *Department of Biochemistry and Molecular Biology, Noakhali Science and Technology University, Noakhali 3814, Bangladesh*

Md Simul Bhuiya − *Department of Biochemistry and Molecular Biology, Jahangirnagar University, Savar 1342, Bangladesh*

Morshed Alam − *Department of Biochemistry and Molecular Biology, Jahangirnagar University, Savar 1342, Bangladesh*

Md. Sakib Hossen − *Department of Biochemistry and Molecular Biology, Primeasia University, Banani 1213, Bangladesh*

Mahruba Sultana Niloy − *Department of Biochemistry and Molecular Biology, Jahangirnagar University, Savar 1342, Bangladesh*

Mohammad Mahfuz Ali Khan Shawan − *Department of Biochemistry and Molecular Biology, Jahangirnagar University, Savar 1342, Bangladesh;* orcid.org/0000-0002-5451-2242

Sheikh Manjura Hoque − *Material Science Division, Atomic Energy Centre, Dhaka 1000, Bangladesh;* orcid.org/0000-0002-4233-9374

Complete contact information is available at: https://pubs.acs.org/10.1021/acsomega.3c00148

https://doi.org/10.1021/acsomega.3c00148
ACS Omega 2023, 8, 15152−15159

Author Contributions

Conceptualization: M.S.S., M.A.H.; nanoparticle synthesis: M.S.S., S.M.H.; experimentation: M.F.U., M.S.S., M.A., M.S.B., M.A.H.; data analysis and diagram: M.S.H., M.S.N., M.A.K.S.; manuscript writing: M.S.S., M.R.M., M.S.N., M.S.H.; manuscript revision and approval: M.S.S., M.A.H. M.S.S. and M.F.U. contributed equally to this work.

Notes

The authors declare no competing financial interest.

■ ACKNOWLEDGMENTS

The project was partially supported by UGC-funded research project (fiscal year 2017−2018) (Regi/Prosha/2114(189), Govt. of Bangladesh, and NST Fellowship (fiscal year 2020−2021), Ministry of Science and Technology, Govt. of Bangladesh. The authors thank the Wazed Mia Science Research Centre (WMSRC), Jahangirnagar University, for allowing use of their facilities to measure iron content. The authors are also thankful to the School of Data and Sciences Course Waiver for Research Policy of Brac University, Bangladesh. The authors thank ES lab, National Brain Research Centre (NBRC), India for supporting the MTS assay.

■ REFERENCES

(1) Srinivasan, S. Y.; Paknikar, K. M.; Bodas, D.; Gajbhiye, V. Applications of cobalt ferrite nanoparticles in biomedical nanotechnology. *Nanomedicine* **2018**, *13* (10), 1221−1238.

(2) Ahmad, F.; Zhou, Y. Pitfalls and Challenges in Nanotoxicology: A Case of Cobalt Ferrite (CoFe2O4) Nanocomposites. *Chem. Res. Toxicol.* **2017**, *30* (2), 492−507.

(3) Panda, J.; Das, S.; Kumar, S.; Tudu, B.; Sarkar, R. Investigation of antibacterial, antioxidant, and anticancer properties of hydrothermally synthesized cobalt ferrite nanoparticles. *Appl. Phys. A: Mater. Sci. Process.* **2022**, *128* (7), 562.

(4) Shakil, M. S.; Mahmud, K. M.; Sayem, M.; Niloy, M. S.; Halder, S. K.; Hossen, M. S.; Uddin, M. F.; Hasan, M. A. Using Chitosan or Chitosan Derivatives in Cancer Therapy. *Polysaccharides* **2021**, *2* (4), 795−816.

(5) Shakil, M. S.; Bhuiya, M. S.; Morshed, M. R.; Babu, G.; Niloy, M. S.; Hossen, M. S.; Islam, M. A. Cobalt Ferrite Nanoparticle's Safety in Biomedical and Agricultural Applications: A Review of Recent Progress. *Curr. Med. Chem.* **2023**, *30* (15), 1756−1775.

(6) Shakil, M. S.; Hasan, M. A.; Uddin, M. F.; Islam, A.; Nahar, A.; Das, H.; Khan, M. N. I.; Dey, B. P.; Rokeya, B.; Hoque, S. M. In Vivo Toxicity Studies of Chitosan-Coated Cobalt Ferrite Nanocomplex for Its Application as MRI Contrast Dye. *ACS Appl. Bio Mater.* **2020**, *3* (11), 7952−7964.

(7) Dugershaw, B. B.; Aengenheister, L.; Hansen, S. S. K.; Hougaard, K. S.; Buerki-Thurnherr, T. Recent insights on indirect mechanisms in developmental toxicity of nanomaterials. *Part Fibre Toxicol* **2020**, *17* (1), 31.

(8) Di Bona, K. R.; Xu, Y.; Ramirez, P. A.; DeLaine, J.; Parker, C.; Bao, Y.; Rasco, J. F. Surface charge and dosage dependent potential developmental toxicity and biodistribution of iron oxide nanoparticles in pregnant CD-1 mice. *Reproductive Toxicology* **2014**, *50*, 36−42.

(9) Di Bona, K. R.; Xu, Y.; Gray, M.; Fair, D.; Hayles, H.; Milad, L.; Montes, A.; Sherwood, J.; Bao, Y.; Rasco, J. F. Short- and Long-Term Effects of Prenatal Exposure to Iron Oxide Nanoparticles: Influence of Surface Charge and Dose on Developmental and Reproductive Toxicity. *International Journal of Molecular Sciences* **2015**, *16* (12), 30251−68.

(10) Noori, A.; Parivar, K.; Modaresi, M.; Messripour, M.; Yousefi, M. H.; Amiri, G. R. Effect of magnetic iron oxide nanoparticles on pregnancy and testicular development of mice. *African Journal of Biotechnology* **2011**, *10* (7), 1221−1227.

(11) Kong, L.; Gao, X.; Zhu, J.; Cheng, K.; Tang, M. Mechanisms involved in reproductive toxicity caused by nickel nanoparticle in female rats. *Environmental Toxicology* **2016**, *31* (11), 1674−1683.

(12) Kong, L.; Tang, M.; Zhang, T.; Wang, D.; Hu, K.; Lu, W.; Wei, C.; Liang, G.; Pu, Y. Nickel nanoparticles exposure and reproductive toxicity in healthy adult rats. *International Journal of Molecular Sciences* **2014**, *15* (11), 21253−69.

(13) deSouza, R. M.; Wallace, D.; Costa, M. L.; Krikler, S. J. Transplacental passage of metal ions in women with hip resurfacing: no teratogenic effects observed. *Hip International* **2012**, *22* (1), 96−9.

(14) Awaad, A.; Seleem, A. A. Histochemical changes in neonatal liver caused by vaginal instillation of magnetic nanoparticles in pregnant mice. *Biotechnic & Histochemistry* **2016**, *91* (1), 48−62.

(15) Bourrinet, P.; Bengele, H. H.; Bonnemain, B.; Dencausse, A.; Idee, J. M.; Jacobs, P. M.; Lewis, J. M. Preclinical safety and pharmacokinetic profile of ferumoxtran-10, an ultrasmall superparamagnetic iron oxide magnetic resonance contrast agent. *Investigative Radiology* **2006**, *41* (3), 313−24.

(16) Pinto, S. R.; Helal-Neto, E.; Paumgartten, F.; Felzenswalb, I.; Araujo-Lima, C. F.; Martinez-Manez, R.; Santos-Oliveira, R. Cytotoxicity, genotoxicity, transplacental transfer and tissue disposition in pregnant rats mediated by nanoparticles: the case of magnetic core mesoporous silica nanoparticles. *Artificial Cells, Nanomedicine, and Biotechnology* **2018**, *46* (sup2), 527−538.

(17) Eisa, A. A. A.; Aboelghar, G. E.; Ammar, I. M.; Metwally, H. G.; Arafa, S. S. Teratogenic effects induced by chitosan oligosaccharide in Wistar female rat Rattus norvegicus. *Environmental Science and Pollution Research* **2018**, *25* (10), 9371−9379.

(18) Park, M. R.; Gurunathan, S.; Choi, Y. J.; Kwon, D. N.; Han, J. W.; Cho, S. G.; Park, C.; Seo, H. G.; Kim, J. H. Chitosan nanoparticles cause pre- and postimplantation embryo complications in mice. *Biol. Reprod.* **2013**, *88* (4), 88.

(19) Choi, Y. J.; Gurunathan, S.; Kim, D.; Jang, H. S.; Park, W. J.; Cho, S. G.; Park, C.; Song, H.; Seo, H. G.; Kim, J. H. Rapamycin ameliorates chitosan nanoparticle-induced developmental defects of preimplantation embryos in mice. *Oncotarget* **2016**, *7* (46), 74658−74677.

(20) Li, A. P.; Bode, C.; Sakai, Y. A novel in vitro system, the integrated discrete multiple organ cell culture (IdMOC) system, for the evaluation of human drug toxicity: comparative cytotoxicity of tamoxifen towards normal human cells from five major organs and MCF-7 adenocarcinoma breast cancer cells. *Chemico-biological interactions* **2004**, *150* (1), 129−36.

(21) Bandyopadhyay Neogi, S.; Roy, D. K.; Sachdeva, A. K.; Sharma, R.; Gupta, R.; Ganguli, A. Evidence of prenatal toxicity of herbal based indigenous formulations for sex selection in rat models. *J. Tradit. Complementary Med.* **2021**, *11* (1), 9−15.

(22) Wang, C.; Lu, J.; Zhou, L.; Li, J.; Xu, J.; Li, W.; Zhang, L.; Zhong, X.; Wang, T. Effects of Long-Term Exposure to Zinc Oxide Nanoparticles on Development, Zinc Metabolism and Biodistribution of Minerals (Zn, Fe, Cu, Mn) in Mice. *PloS one* **2016**, *11* (10), No. e0164434.

(23) Ohkawa, H.; Ohishi, N.; Yagi, K. Assay for lipid peroxides in animal tissues by thiobarbituric acid reaction. *Analytical biochemistry* **1979**, *95* (2), 351−8.

(24) Hashimoto, M.; Shahdat, M. H.; Shimada, T.; Yamasaki, H.; Fujii, Y.; Ishibashi, Y.; Shido, O. Relationship between age-related increases in rat liver lipid peroxidation and bile canalicular plasma membrane fluidity. *Experimental gerontology* **2001**, *37* (1), 89−97.

(25) Nahar, A.; Hanium Maria, K.; Liba, S. I.; Anwaruzzaman, M.; Khan, M. N. I.; Islam, A.; Choudhury, S.; Hoque, S. M. Surface-modified CoFe2O4 nanoparticles using Folate-Chitosan for cytotoxicity Studies, hyperthermia applications and Positive/Negative contrast of MRI. *J. Magn. Magn. Mater.* **2022**, *554*, 169282.

(26) Shakil, M. S.; Rana, Z.; Hanif, M.; Rosengren, R. J. Key considerations when using the sulforhodamine B assay for screening novel anticancer agents. *Anti-cancer drugs* **2022**, *33* (1), 6−10.

https://doi.org/10.1021/acsomega.3c00148
ACS Omega 2023, 8, 15152−15159

(27) Teng, C.; Jiang, C.; Gao, S.; Liu, X.; Zhai, S. Fetotoxicity of Nanoparticles: Causes and Mechanisms. *Nanomaterials (Basel)* **2021**, *11* (3), 791.
(28) Bongaerts, E.; Nawrot, T. S.; Van Pee, T.; Ameloot, M.; Bove, H. Translocation of (ultra)fine particles and nanoparticles across the placenta; a systematic review on the evidence of in vitro, ex vivo, and in vivo studies. *Particle and Fibre Toxicology* **2020**, *17* (1), 56.
(29) Yu, W. J.; Son, J. M.; Lee, J.; Kim, S. H.; Lee, I. C.; Baek, H. S.; Shin, I. S.; Moon, C.; Kim, S. H.; Kim, J. C. Effects of silver nanoparticles on pregnant dams and embryo-fetal development in rats. *Nanotoxicology* **2014**, *8*, 85−91.
(30) Lee, J.; Jeong, J. S.; Kim, S. Y.; Park, M. K.; Choi, S. D.; Kim, U. J.; Park, K.; Jeong, E. J.; Nam, S. Y.; Yu, W. J. Titanium dioxide nanoparticles oral exposure to pregnant rats and its distribution. *Part Fibre Toxicol* **2019**, *16* (1), 31.
(31) Kim, J. S.; Yoon, T. J.; Yu, K. N.; Kim, B. G.; Park, S. J.; Kim, H. W.; Lee, K. H.; Park, S. B.; Lee, J. K.; Cho, M. H. Toxicity and tissue distribution of magnetic nanoparticles in mice. *Toxicol. Sci.* **2006**, *89* (1), 338−47.
(32) Liu, Y.-k.; Xu, H.; Liu, F.; Tao, R.; Yin, J. Effects of serum cobalt ion concentration on the liver, kidney and heart in mice. *Orthopaedic Surgery* **2010**, *2* (2), 134−140.
(33) Pradhan, P.; Giri, J.; Samanta, G.; Sarma, H. D.; Mishra, K. P.; Bellare, J.; Banerjee, R.; Bahadur, D. Comparative evaluation of heating ability and biocompatibility of different ferrite-based magnetic fluids for hyperthermia application. *J. Biomed. Mater. Res.* **2007**, *81B* (1), 12−22.
(34) Bassiony, H.; El-Ghor, A. A.; Salaheldin, T. A.; Sabet, S.; Mohamed, M. M. Tissue Distribution, Histopathological and Genotoxic Effects of Magnetite Nanoparticles on Ehrlich Solid Carcinoma. *Biological trace element research* **2022**, *200* (12), 5145−5158.
(35) Zhang, J.; Liu, S.; Han, J.; Wang, Z.; Zhang, S. On the developmental toxicity of silver nanoparticles. *Materials & Design* **2021**, *203*, 109611.
(36) Ahmad, F.; Zhou, Y. Pitfalls and Challenges in Nanotoxicology: A Case of Cobalt Ferrite (CoFe(2)O(4)) Nanocomposites. *Chem. Res. Toxicol.* **2017**, *30* (2), 492−507.
(37) Akhtar, K.; Javed, Y.; Jamil, Y.; Muhammad, F. Functionalized cobalt ferrite cubes: toxicity, interactions and mineralization into ferritin proteins. *Applied Nanoscience* **2020**, *10* (9), 3659−3674.
(38) Katuli, K. K.; Massarsky, A.; Hadadi, A.; Pourmehran, Z. Silver nanoparticles inhibit the gill Na^+/K^+-ATPase and erythrocyte AChE activities and induce the stress response in adult zebrafish (Danio rerio). *Ecotoxicology and environmental safety* **2014**, *106*, 173−80.
(39) Katz, A. I. Renal Na-K-ATPase: its role in tubular sodium and potassium transport. *American journal of physiology* **1982**, *242* (3), F207−19.
(40) Fennell, T. R.; Mortensen, N. P.; Black, S. R.; Snyder, R. W.; Levine, K. E.; Poitras, E.; Harrington, J. M.; Wingard, C. J.; Holland, N. A.; Pathmasiri, W.; Sumner, S. C. Disposition of intravenously or orally administered silver nanoparticles in pregnant rats and the effect on the biochemical profile in urine. *J. Appl. Toxicol* **2017**, *37* (5), 530−544.
(41) Akhtar, S.; An, W.; Niu, X.; Li, K.; Anwar, S.; Maaz, K.; Maqbool, M.; Gao, L. Toxicity of PEG-Coated CoFe(2)O(4) Nanoparticles with Treatment Effect of Curcumin. *Nanoscale Res. Lett.* **2018**, *13* (1), 52.
(42) Poulsen, M. S.; Mose, T.; Maroun, L. L.; Mathiesen, L.; Knudsen, L. E.; Rytting, E. Kinetics of silica nanoparticles in the human placenta. *Nanotoxicology* **2015**, *9*, 79−86.
(43) Yarjanli, Z.; Ghaedi, K.; Esmaeili, A.; Rahgozar, S.; Zarrabi, A. Iron oxide nanoparticles may damage to the neural tissue through iron accumulation, oxidative stress, and protein aggregation. *BMC neuroscience* **2017**, *18* (1), 51.
(44) Ahmad, F.; Zhou, Y. Pitfalls and Challenges in Nanotoxicology: A Case of Cobalt Ferrite (CoFe2O4) Nanocomposites. *Chemical research in toxicology* **2017**, *30* (2), 492−507.
(45) Albrahim, T.; Alonazi, M. A. Role of Beetroot (Beta vulgaris) Juice on Chronic Nanotoxicity of Silver Nanoparticle-Induced Hepatotoxicity in Male Rats. *Int. J. Nanomedicine* **2020**, *15*, 3471−3482.

https://doi.org/10.1021/acsomega.3c00148
ACS Omega 2023, 8, 15152−15159